0026-895X/09/7505-1096–1107$20.00
MOLECULAR PHARMACOLOGY
Copyright © 2009 The American Society for Pharmacology and Experimental Therapeutics
Mol Pharmacol 75:1096–1107, 2009

Vol. 75, No. 5
54254/3464655
Printed in U.S.A.

Functional Characterization and In Silico Docking of Full and Partial GluK2 Kainate Receptor Agonists

Anne-Marie L. Fay, Christopher R. Corbeil, Patricia Brown, Nicolas Moitessier, and Derek Bowie

Departments of Pharmacology and Therapeutics (A.-M.L.F., P.B., D.B.) and Chemistry (C.R.C., N.M.), McGill University, Montréal, Québec, Canada

Received December 18, 2008; accepted February 18, 2009

ABSTRACT

Two structural models have been developed to explain how agonist binding leads to ionotropic glutamate receptor (iGluR) activation. At α-amino-3-hydroxy-5-methyl-4-isoxazolepropionic acid (AMPA) iGluRs, full and partial agonists close the agonist-binding domain (ABD) to different degrees whereas agonist-induced domain closure is apparently fixed at *N*-methyl-D-aspartate receptors. Although kainate (KA) iGluRs are thought to behave like AMPA receptors, the issue has not been formally tested because of the paucity of available receptor agonists. Here we identify a series of structurally related full and partial agonists at GluK2 (formerly GluR6) KARs and predict their docking mode using the in silico ligand-docking program FITTED. As expected, the neurotransmitter L-Glu behaved as a full agonist but modest reduction (e.g., L-serine or L-aspartate) or elongation (e.g., L-α-aminoadipate) in chain length generated weak partial agonists. It is noteworthy that in silico ligand-docking predicted that most partial agonists select for the closed and not, as expected, the open or intermediate conformations of the GluK2 ABD. Experiments using concanavalin-A to directly report conformations in the intact GluK2 receptor support this prediction with the full agonist, L-Glu, indistinguishable in this regard from weak partial agonists, D- and L-Asp. Exceptions to this were KA and domoate, which failed to elicit full closure as a result of steric hindrance by a key tyrosine residue. Our data suggest that alternative structural models need to be considered to describe agonist behavior at KARs. Finally, our study identifies the responsiveness to several neurotransmitter candidates establishing the possibility that endogenous amino acids other than L-Glu may regulate native KARs at central synapses.

iGluRs mediate the vast majority of excitatory neurotransmission in the mammalian brain and have been implicated in numerous CNS disorders (Bowie, 2008). Given this, much research has focused on their structure-function properties because, among other benefits, it provides a rational approach to drug discovery. Insight into their structure was first advanced by homology modeling using the bilobed domain of bacterial amino acid binding proteins as a template (Stern-Bach et al., 1994). Subsequently, the agonist-binding domain (ABD) of the GluA2 (Collingridge et al., 2009) (formerly GluR2 or GluRB) AMPAR was crystallized, revealing the predicted clamshell-like structure of globular domains 1 and 2 that close upon agonist binding (Armstrong and Gouaux, 2000). Since then, a similar approach has permitted the atomic resolution of ABDs of all iGluR family members, including the KAR (Mayer, 2005; Nanao et al., 2005), NMDAR (Inanobe et al., 2005), and, more recently, the δ-2 orphan iGluR (Naur et al., 2007). From these studies, two structural models of agonist behavior have emerged. At the NR1 NMDAR subunit, full and partial agonists differ little in the conformational change they elicit in the ABD (Inanobe et al., 2005). In contrast, at AMPARs, agonist efficacy is thought to reside in the conformations adopted by the ABD, full agonists more effective at promoting domain closure than partial agonists (Armstrong and Gouaux, 2000; Jin et al., 2003).

Although KARs are thought to behave like AMPARs, the structural basis of agonist efficacy of this receptor family has

This work was supported by the Canadian Institutes of Health Research (CIHR); the Fonds de la Recherche en Santé du Québec; the CIHR-funded Chemical Biology program; and a Canada Research Chair award.

Article, publication date, and citation information can be found at http://molpharm.aspetjournals.org.

doi:10.1124/mol.108.054254.

ABBREVIATIONS: iGluR, ionotropic glutamate receptor; CNS, central nervous system; ABD, agonist-binding domain; AMPA, α-amino-3-hydroxy-5-methyl-4-isoxazolepropionic acid; AMPAR, AMPA receptor; KA, kainate; KAR, kainate receptor; Dom, domoate; NMDA, *N*-methyl-D-aspartate; NMDAR, *N*-methyl-D-aspartate receptor; QA, quisqualic acid; SYM 2081, (2*S*,4*R*)-4-methylglutamic acid; BAPTA, 1,2-bis(2-aminophenoxy)-ethane-*N*,*N*,*N*′,*N*′-tetraacetic acid; RMSD, root-mean-square deviation; SOS, L-serine-*O*-sulfate; L-Cys, L-cysteic acid; SSC, *S*-sulfo-L-cysteic acid; HCSA, L-homocysteine sulfinic acid; HC, L-homocysteic acid; Con-A, concanavalin-A; CNQX, 6-cyano-7-nitroquinoxaline-2,3-dione; PhTX, philanthotoxin; FITTED, Flexibility Induced Through Targeted Evolutionary Description.

not been firmly established for several reasons. First and foremost, there are fewer agonist-bound crystal structures available to make the comparison. To date, the ABD of GluK1 and/or GluK2 bound by the full agonist L-Glu and partial agonists KA and domoic acid (Dom) have been resolved at atomic resolution (Mayer, 2005; Nanao et al., 2005). Other structures for quisqualic acid (QA) and SYM 2081 have also been described (Mayer, 2005) but it is not yet clear whether they act as full or partial agonists. Second, the extent of domain closure elicited by the full agonist, L-Glu, differs from partial agonist, KA, by only 3° (Mayer, 2005), which is modest in comparison with the effect of the same agonists at AMPARs (e.g., L-Glu versus KA, 8° difference) (Armstrong and Gouaux, 2000). An added complication is that the apo state of the KAR ABD has yet to be resolved; therefore, the extent of domain closure is given with respect to the GluA2 AMPAR apo state. Third and finally, KARs require external anions and cations as well as the neurotransmitter L-glutamate for activation (Wong et al., 2006), a property not shared by AMPARs (Bowie, 2002). Given this, it is possible that the degree of activation of KARs is shaped not only by the agonist molecule but also by external ions.

Here, we have tested the functionality of a range of L-Glu analogs as a first step in understanding the structural basis of agonist behavior at KARs. To complement this data, we also used the in silico ligand-docking program FITTED to predict the conformation of the ABD preferred by each agonist. It is noteworthy that this combined approach suggests unexpectedly that most partial agonists select for the closed and not the open or intermediate conformation of GluK2 ABD. This finding suggests that agonist efficacy at KARs may not be solely determined by the extent of closure in the GluK2 ABD; therefore, alternative structural models may need to be considered.

Materials and Methods

Cell Culture and Transfection. Techniques used to culture and transfect mammalian cells to express GluR6 KARs have been described in detail elsewhere (Bowie, 2002). In brief, tsA201 cells, a transformed human embryonic kidney 293 cell line stably expressing a simian virus 40 temperature-sensitive T antigen (provided by R. Horn, Jefferson Medical College, Philadelphia, PA) were maintained at a confluence of 70 to 80% in minimal essential medium with Earle's salts, 2 mM glutamine, and 10% fetal bovine serum supplemented with penicillin (100 units/ml) and streptomycin (100 μg/ml). After plating at low density (2×10^4 cells/ml) on plastic dishes, cells were transfected with cDNA encoding unedited rat glutamate receptor subunit 6 using the calcium phosphate technique as described previously (Bowie, 2002). The cDNA for enhanced green fluorescent protein (S65T mutant) was routinely cotransfected to identify transfected cells. In this and all subsequent publications from our laboratory, we adopt the recommended change to iGluR nomenclature (Collingridge et al., 2009). Consequently, GluR6 will be referred to as GluK2 and the GluR-B or GluR2 AMPAR subunit as GluA2.

Electrophysiological Solutions and Techniques. All ligands tested in this study were dissolved in external solutions containing 150 mM NaCl and 5 mM HEPES with low concentrations of $CaCl_2$ and $MgCl_2$ (0.1 mM each) to avoid divalent block. For dose-response relationships to D- and L-Asp (Fig. 3D), however, agonists were applied at concentrations (i.e., >100 mM) that would cause a shift in reversal potential as a result of changes in the driving force for the main permeant ion, Na^+. To avoid this, the ionic strength of all solutions was increased to 200 mM, with the desired agonist concentration balanced by the appropriate amount of NaCl. All concentrated ligand solutions were adjusted to pH 7.3 with NaOH before being stored at −20°C. Saturating agonist concentrations chosen for L-Glu (10 mM), kainate (1 mM), domoate (50 μM) were at least 5-fold higher than published EC_{50} values at GluK2 receptors. We confirmed empirically that these concentrations were saturating by doubling the agonist concentration in each case and observing that peak response amplitudes were unchanged. For sulfur-containing amino acids, QA, SYM 2081, and L-α-aminoadipate, saturating levels were determined empirically by increasing concentrations until a maximal response was observed. In cases in which millimolar concentrations of agonist were required for activation (e.g., 40 mM L-cysteic acid), the reported response amplitudes were corrected for the shift in the reversal potential observed. Internal pipette solution contained 115 mM NaCl, 10 mM NaF, 5 mM HEPES, 5 mM Na_4BAPTA, 0.5 mM $CaCl_2$, 1 mM $MgCl_2$, and 10 mM Na_2ATP to chelate endogenous polyamines. The pH and osmotic pressure of internal and external solutions were adjusted to 7.3 and 295 mOsmol/kg, respectively. Concanavalin-A (Con-A) (Sigma, St. Louis) was prepared in glucose free saline solution and filtered (0.2 μm filter, Corning) immediately before use as described previously (Bowie et al., 2003). All recordings were performed with an Axopatch 200B amplifier (Axon Instruments Inc., CA) using thin-walled borosilicate glass pipettes (2–5 MΩ) coated with dental wax to reduce electrical noise. Control and agonist solutions were rapidly applied to outside-out patches excised from transfected tsA201 cells as described previously (Bowie, 2002). Solution exchange (10–90% rise-time = 25–50 μs) was determined routinely at the end of the experiment by measuring the liquid junction current (or exchange current) between the control and agonist-containing solution in which total Na^+-content was reduced by 5%. Current records were filtered at 5 kHz, digitized at 25 to 50 kHz and series resistances (3–10 MΩ) compensated by 95%. Most recordings were performed at −20 mV membrane potential to ensure adequate voltage clamp control of peak currents. Data acquisition was performed using pClamp9 software (Molecular Devices, Sunnyvale, CA). All experiments were carried out at room temperature (22 to 23°C).

Overview of the Docking Program FITTED. Conformational changes in the ligand-binding domain of iGluRs have been investigated through X-ray crystallography. Previous X-ray data have revealed two fundamental features pertaining to the ligand-binding domain of iGluRs, which has made it difficult to accurately model these proteins. First, the model must allow for protein flexibility, because it is well established that the ligand-binding domain can adopt a range of degree of clamshell closure. Moreover, given that water molecules have been shown to play a key role in stabilizing the ligand in the binding cleft of both AMPA and KARs (Mayer, 2005), the docking program would have to allow for displacement and movement of waters. Until recently, docking software that simultaneously accounted for these features in their search algorithm was not available. However, the development of a genetic algorithm based docking program called FITTED 2.0 (Flexibility Induced Through Targeted Evolutionary Description), which performs all these functions has recently been described previously (Corbeil et al., 2007). This docking tool can uniquely accommodate for displaceable bridging water molecules, whereas treating the ligand/protein as a realistically dynamic system, and therefore provides the most appropriate docking approach to investigate iGluRs. For data shown in this study, we used FITTED version 2.0 using the semiflexible docking option with displaceable waters and, in each case, the pharmacophore-oriented docking function was used (Corbeil et al., 2007).

Protein and Ligand Structure Preparation before Docking. The X-ray structures of GluK2 complexes were retrieved from the Protein Data Bank (codes 1s50, 1s7y, 1sd3, 1s9t, 1tt1, 1yae) and hydrogen atoms were added with their position optimized through energy minimization. The result was visually inspected, as described previously to ensure the optimum hydrogen bond network (Corbeil et al., 2007). Six bridging water molecules found to be conserved

throughout most of the ligand-protein complexes were retained for the docking study. All protein structures were prepared using ProCESS (a module of FITTED), and the ligands were fully ionized and prepared with SMART (a module of FITTED) (Corbeil et al., 2007).

Docking Amino Acid Ligands using FITTED. The data obtained from docking experiments are summarized in Table 1. Six protein structures initially resolved with five different agonists were used as input files [i.e., 1s7y (L-Glu), 1s9t (QA), 1sd3 (SYM 2081), 1tt1 (kainate), 1yae_a (domoate, conformation 1), and 1yae_b (domoate, conformation 2)]. All the original Protein Data Bank files pertain to KAR dimer structures solved with different ligands (Mayer, 2005) with the exception of 1yae, which was solved as a hexamer (Nanao et al., 2005). To compare GluK2 monomers within a given polymer, protein superimposition was achieved by aligning the α-carbons of the residues found with at least one atom within 10 Å from the ligand. With the exception of 1yae, all the monomers within a given polymer were identical. Therefore, only one of the monomers/dimer was retained for the docking studies. As for 1yae, two monomers (1yae_a and 1yae_b) were retained as input files to allow for greater protein fluctuations within the binding pocket. The five agonists (L-Glu, QA, SYM 2081, KA, and domoate) were docked using six protein structures as input files (1s7y, 1s9t, 1sd3, 1tt1, 1yae_a, and 1yae_b). As previously reported, comparison of the crystal structures reveals three distinct protein conformations that we will refer to as closed, intermediate, and open. Consistent with the identical degree of domain closure observed with the binding of L-Glu (1s7y), SYM 2081 (1sd3), or QA (1s9t) at GluK2 crystals, the computed root-mean-square deviation (RMSD) between the active site of all three protein structures were small (1s7y and 1sd3, 0.24 Å; 1s7y and 1s9t, 0.46 Å; 1sd3 and 1s9t, 0.51 Å). For the remainder of the text, the term "closed" conformation will be used to refer to any of these three protein conformations. In agreement with crystallographic studies (Nanao et al., 2005), the "open" state will denote the conformation observed with domoate-bound crystals (RMSD between 1s7y and 1yae, 1.6 Å). Finally, the conformation adopted by the kainate-bound GluR6 crystal conformation will be termed "intermediate" (RMSD between 1s7y and 1tt1, 0.91 Å).

We assessed the validity of FITTED 2.0 for GluK2 KARs in several ways. First, we performed statistical analysis comparing the ligand bound in the actual crystal structures with the docked ligand predicted by FITTED. A ligand pose was considered successfully docked when the RMSD relative to the ligand bound in the actual crystal structure was below 2.0 Å (Table 1) (Corbeil et al., 2007). Second, the protein structure was considered to be accurately selected when the population favored that specific protein conformation over others (Corbeil et al., 2007). Third, we compared the number and position of water molecules in the crystal structure with that predicted by FITTED. In all cases, FITTED correctly predicted the number and position of water molecules. For each pose, FITTED used the RankScore function to yield a docking score, an estimation of the free energy of binding including entropic contributions (Table 1). It is noteworthy that although the scoring function has been trained to reproduce free energies of binding, the accuracy level is not high enough to make highly accurate predictions within two orders of magnitude in K_i. In addition, the apparent agonist affinity (see Fig. 3) is not governed only by the free energy of agonist binding but also by multiple aspects of ion-channel behavior that include channel gating properties and desensitization. A minimum set of 10 runs was carried out for each ligand (Corbeil et al., 2007). An initial population of 500 was enough for docking of all GluK2 KAR ligands to reach the convergence criterion. Moreover, a maximum of 500 generations was used to reach convergence for each ligand.

Assumptions of Molecular Docking Strategy. To perform molecular ligand docking experiments, four assumptions were made. First, our modeling strategy pertained to transposing the information obtained from resolved crystal with the behavior of the mature receptor under physiological conditions. Our electrophysiological recordings from GluK2 KARs were performed under physiological pH 7.3 to 7.4, whereas most of the GluK2 S1S2 isolated cores were crystallized under conditions that were significantly more acidic (ranging from 4.0 to 6.5). To assess the effect (if any) of these pH fluctuations, we compared the two GluK2 KAR crystals in complex with L-Glu that were cocrystallized at distinct pH (1s50, pH 8.0; 1s7y, pH 4.8) (Mayer, 2005). Visual inspection of the superimposed protein-ligand complexes revealed no significant differences between the two structures. We therefore used the 1s7y structure and did not further consider 1s50 in our analysis. Second, our modeling experiments assumed that all the amino acids tested bind in the same cavity between the S1S2 domains (i.e., the orthosteric site) as previously reported for other ligands cocrystallized with GluK2 KARs. Third, because the apo state of GluK2 KARs has yet to be resolved, the degree of domain closure of the agonist-binding domain was obtained in comparison with the apo state of GluA2 AMPA receptor. Fourth, we have assumed that L-Glu analogs bind to one of the three known GluK2 conformations identified through X-ray crystallography (open, intermediate, and closed). The computed RMSD between the active sites of structures for L-Glu (1s7y), SYM 2081 (1sd3) and QA (1s9t) were small (1s7y and 1sd3, 0.24 Å; 1s7y and 1s9t, 0.46 Å;

TABLE 1

Functional and structural properties of GluK2 KAR agonists

Functional properties of responses elicited by the sixteen GluK2 receptor agonists examined in this study. Structural information obtained with FITTED are also provided. All data are expressed as the mean ± S.E.M.

Agonist, Concentration Range	Peak		Ligand Category	Conformation		RMSD	Docking Score (FITTED)
				Selected (FITTED)	Experimental (Crystallography)		
	%	*n*					
L-Glu,10 mM	100	43	Full	Closed	Closed	0.34	−5.73
SYM 2081, 1–3 mM	102.0 ± 7.7	3	Full	Closed	Closed	0.24	−6.52
QA, 1–3 mM	90.0 ± 1.1	3	Full	Closed	Closed	2.0	−8.70
L-Cys, 10–60 mM	73.6 ± 1.9	4	Partial	Closed			−5.60
SSC, 1–2 mM	64.1 ± 7.6	5	Partial	Closed			−8.06
HCSA, 10–40 mM	58.0 ± 5.4	5	Partial	Closed			−6.84
KA, 1–3 mM	39.1 ± 2.0	10	Partial	Intermediate	Intermediate	0.46	−8.33
HC, 10–40 mM	34.4. ± 3.4	8	Partial	Closed			−6.62
CSA, 10–40 mM	31.72 ± 3.75	3	Partial	Closed			−6.97
Dom, 50–150 μM	15.3 ± 1.9	8	Partial	Open	Open	1.2	−8.88
L-Aminoadipate, 10–40 mM	14.05 ± 0.19	4	Partial	Closed			−6.70
D-Asp, 10 mM	3.6 ± 1.15	6	Partial	Closed			−6.29
L-Asp, 10 mM	0.95 ± 0.39	5	Partial	Closed			−5.13
SOS, 1–20 mM	0.52 ± 0.7	3	Partial	Closed			−7.24
L-Ser, 10 mM	0.26 ± 0.3	3	Partial	Closed			−5.01
D-Ser, 10 mM	0.05 ± 0.5	3	Partial	Closed			−4.96

1sd3 and 1s9t, 0.51 Å), and therefore their domain closure was considered indistinguishable in agreement with previous structural analysis (Mayer, 2005).

Results

L-Glu Analogs Exhibit a Wide Range of Agonist Activity at GluK2 Receptors. In an effort to identify receptor ligands that exhibit the full range of agonist behavior, we studied the kinetic properties of a number of commercially available L-Glu analogs (see *Materials and Methods*). In all cases, agonists were applied at saturating concentrations and at frequencies that permit full recovery from desensitization. Figure 1 shows the extended structure of the selected amino acids all of which possess a common L-Glu backbone. We purposely chose this group of amino acids because they would provide information on how agonist efficacy is shaped by changes in chain length, atom substitution, as well as the addition of side groups and/or sulfur groups. Agonist activity of several of these amino acids have been previously reported at AMPARs, NMDARs, and metabotropic glutamate receptors (Patneau and Mayer, 1990; Kingston et al., 1998) but not yet at KARs.

Almost all amino acids tested elicited membrane currents that consisted of a rapidly rising peak response, which declined in the presence of the agonist to a new equilibrium level (Fig. 2 upper, Table 1). In some cases, as with L-serine-*O*-sulfate (SOS) and stereoisomers of serine (Ser) and aspartate (Asp), responses were difficult to resolve because of their small amplitude (even in high-expressing patches), which made detailed kinetic analysis problematic (Figs. 2 and 3). Nevertheless, a wide range of agonist efficacy was observed among all the amino acids tested (Fig. 2, bottom). For example, five sulfur-containing amino acids exhibited the following rank order of efficacy: L-cysteic acid (L-Cys, 40 mM) > *S*-sulfo-L-cysteic acid (SSC; 20 mM) > L-homocysteine sulfinic acid (HCSA; 40 mM) > L-homocysteic acid (HC; 20 mM) > SOS (1 mM) based on peak response amplitude with saturating agonist concentrations (Fig. 2, top). As mentioned above, SOS evoked barely detectable responses demonstrating that even modest changes to the agonist structure has pronounced effects on agonist efficacy (Fig. 2, top). In this case, replacement of the sulfur atom at the ω-position with an oxygen converted the partial agonist, SSC, into the poorly stimulating SOS. Except for SYM2081 and QA, all other

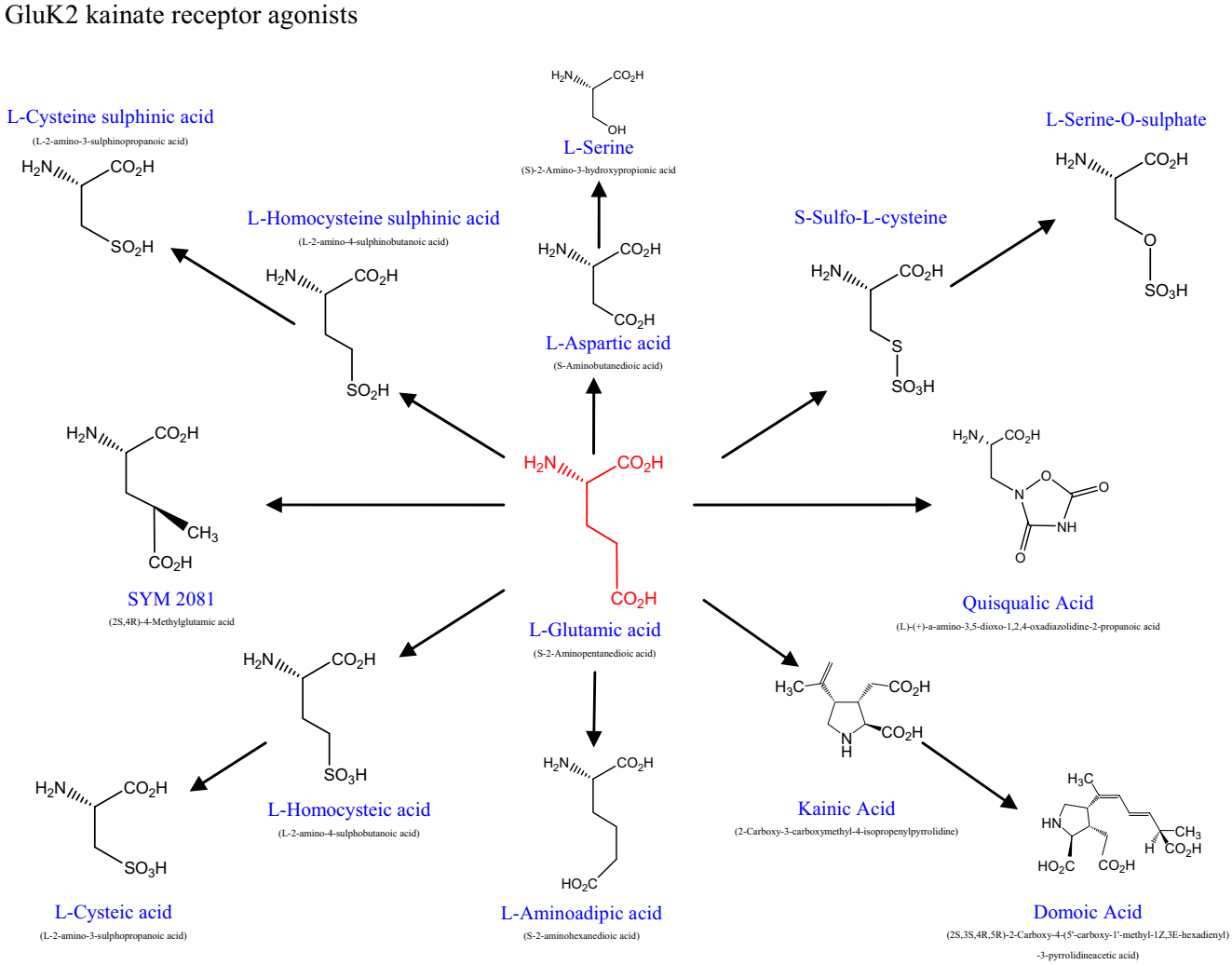

Fig. 1. Extended structure of GluK2 receptor agonists. Schematic diagram showing the extended structure of all the amino acids selected for investigation. All amino acids are structural analogs of L-Glu and thus were chosen purposely to provide information on how changes in chain length, atom substitution, and the addition of side groups and/or sulfur groups affect agonist efficacy. Each structure is identified by both its common and IUPAC nomenclature.

agonists tested were partial agonists because they elicited peak responses smaller than that observed with L-Glu (one sample t test, $p < 0.01$; Fig. 2, bottom). Finally, modest reduction (e.g., L-serine and L-aspartate) or elongation (e.g., L-α-aminoadipate) in chain length of the L-Glu structure generates weak partial agonists suggesting that the KAR ABD is optimized for the binding of this amino acid.

Desensitization Does Not Profoundly Affect Estimates of Peak Response Amplitude. Although solution exchanges performed in this study were rapid, relative rates of activation and desensitization may vary among different agonists. Consequently, agonists designated as poorly conducting (i.e., weak partial agonists) may, in fact, behave as full agonists if studied in the absence of desensitization. To address this issue, we looked more closely at SOS and the stereoisomers (i.e., D and L) of both Asp and Ser, which were ideal for this purpose because these ligands represent the five weakest responding agonists, which, as explained above, may reflect genuine partial agonist activity or result from rapid rates into desensitization. To delineate between these two possibilities, we examined agonist responses after treatment with the plant lectin, concanavalin-A (Con-A).

Although Con-A does not block desensitization or shift apparent agonist affinity, it irreversibly increases current flow through GluK2 KARs (Bowie et al., 2003). We reasoned that this property would permit better resolution of re-

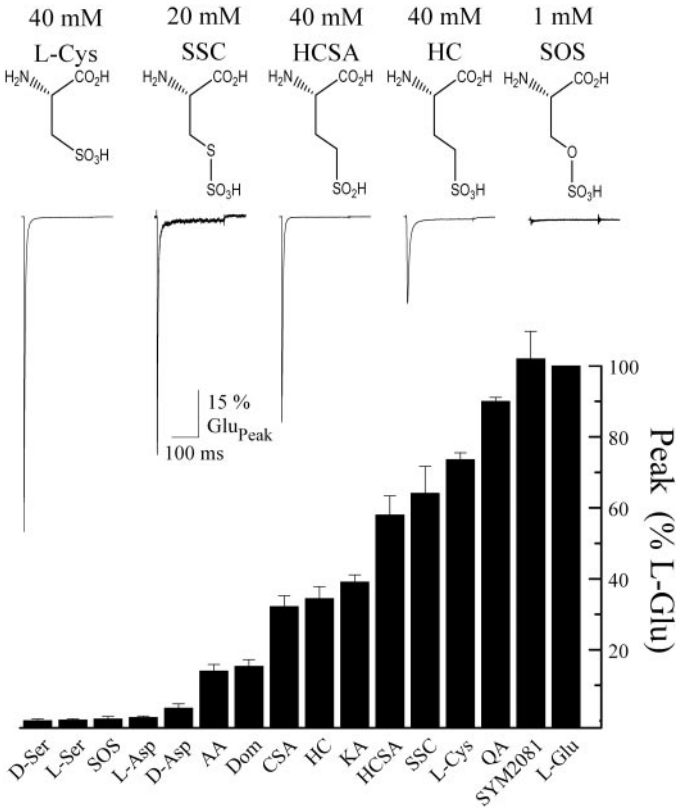

Fig. 2. Response profile of an extended series of GluK2 kainate receptor agonists. Top, structure-function relationship of five sulfur-containing amino acids aligned in order of peak agonist responsiveness. To allow comparison between experiments, membrane currents were normalized to the peak L-Glu response in each recording. Patch numbers were 04622p4 (L-Cys), 04629p2 (HCSA), 060720p1 (HC), 060720p4 (SSC)b, and 04621p1 (SOS). Bottom, summary bar graph comparing the peak response amplitude observed with saturating concentrations of each amino acid (n = 8–43 patch recordings). The data are arranged in increasing order of responsiveness, from very weak partial agonists (stereoisomers of serine and aspartate as well as SOS) to QA, SYM 2081, and L-Glu, which are full agonists. All data are expressed as the mean ± S.E.M.

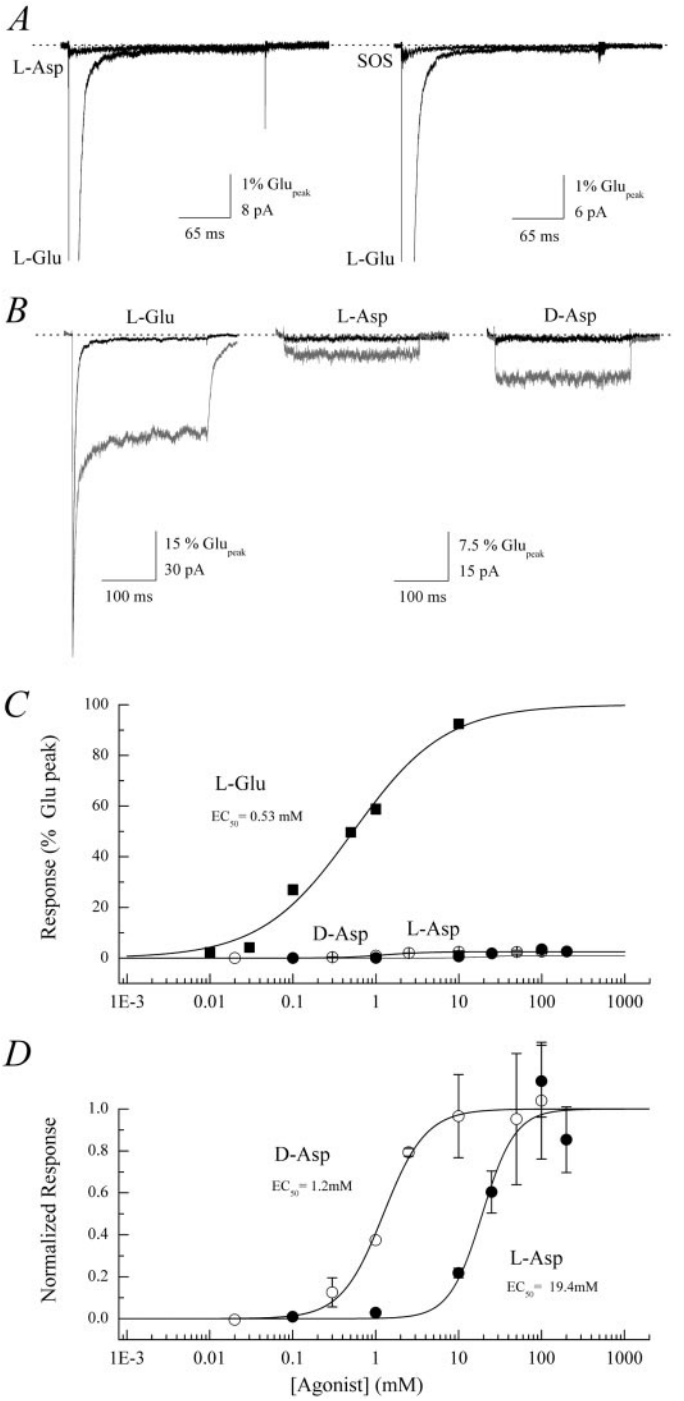

Fig. 3. Stereoisomers of aspartate are partial agonists at GluK2 kainate receptors. A, representative membrane currents elicited by 10 mM L-Glu, 10 mM L-Asp, and 1 mM SOS (patch numbers 080425p2). The dotted line denotes the zero current level. B, typical electrophysiological recordings elicited by 10 mM L-Glu, L-Asp, and D-Asp (10 mM each) before (black line) and after (gray line) Concanavalin-A (3 min) treatment in the same patch (patch number 080425p2). Con-A treatment reveals that both D- and L-Asp elicit rapidly rising, nondesensitizing membrane currents that quickly deactivate upon cessation of the agonist application. C and D, activation curves to L-Glu as well as D- and L-Asp reveal that stereoisomers of Asp are weak partial agonists with significantly lower affinity than with the full agonist L-Glu.

sponses elicited by weakly responding agonists. Before Con-A treatment, typical responses elicited by each of these agonists were small in amplitude, which made accurate analysis of their kinetic properties problematic as shown in Fig. 3A for 10 mM L-Asp and SOS. To allow comparison, membrane currents elicited by the full agonist, L-Glu (10 mM), in the same patch recording are shown superimposed (Fig. 3A). As anticipated, Con-A treatment (10 μM, 3–5 mins) increased current flow through GluK2 receptors activated by SOS and stereoisomers of both Asp and Ser, making it possible to routinely study their peak responses (Fig. 3B). From detailed analysis of the stereoisomers of Asp, two important characteristics of their response were revealed that unequivocally demonstrate that they behave as partial agonists. First, stereoisomers of Asp elicited rapidly rising, nondesensitizing membrane currents showing that these agonists are not weakly responding because of the rapid onset of desensitization (Fig. 3B). Second, construction of activation curves for each agonist revealed that maximal responses in each case were significantly smaller than with L-Glu (Fig. 3C). Compared with the maximal response elicited by L-Glu, responses to saturating concentrations of D- and L-Asp were 2.5 ± 0.1% and 3.0 ± 0.3% (n = 4–6), respectively. In addition, estimated EC_{50} values (Hill coefficient, n_H) for D-Asp and L-Asp were 1.2 ± 0.1 mM (n_H = 1.7 ± 0.3) and 19.4 ± 4.7 mM (n_H = 2.2 ± 1.1), respectively, compared 0.5 ± 0.1 mM (n_H = 0.8 ± 0.1) for L-Glu (Fig. 3, C and D). Taken together, these observations directly demonstrate that D -and L-isomers of Asp elicit responses of small amplitude because they are partial agonists and not due to the rapid onset of desensitization.

In Silico Ligand-Docking Correctly Identifies Conformations Adopted by the Gluk2 Agonist-Binding Domain. To combine this functional data with in silico ligand-docking using FITTED, we first focused on receptor agonists previously cocrystallized with the isolated ligand binding core of GluK2 (Mayer, 2005; Nanao et al., 2005). From electrophysiology recordings, we already identified kainate (1 mM KA) and domoate (50 μM Dom) as partial agonists at GluK2 receptors with L-glutamate (10 mM L-Glu), SYM 2081 (3 mM), and quisqualate (3 mM QA) all behaving as full agonists when applied at saturating concentrations (Fig. 4, A and B). Peak KA and Dom responses were 39.1 ± 2.0% (n = 10) and 15.3 ± 1.9% (n = 8) respectively of the maximal full agonist response (Fig. 4B, Table 1). Previous structural work

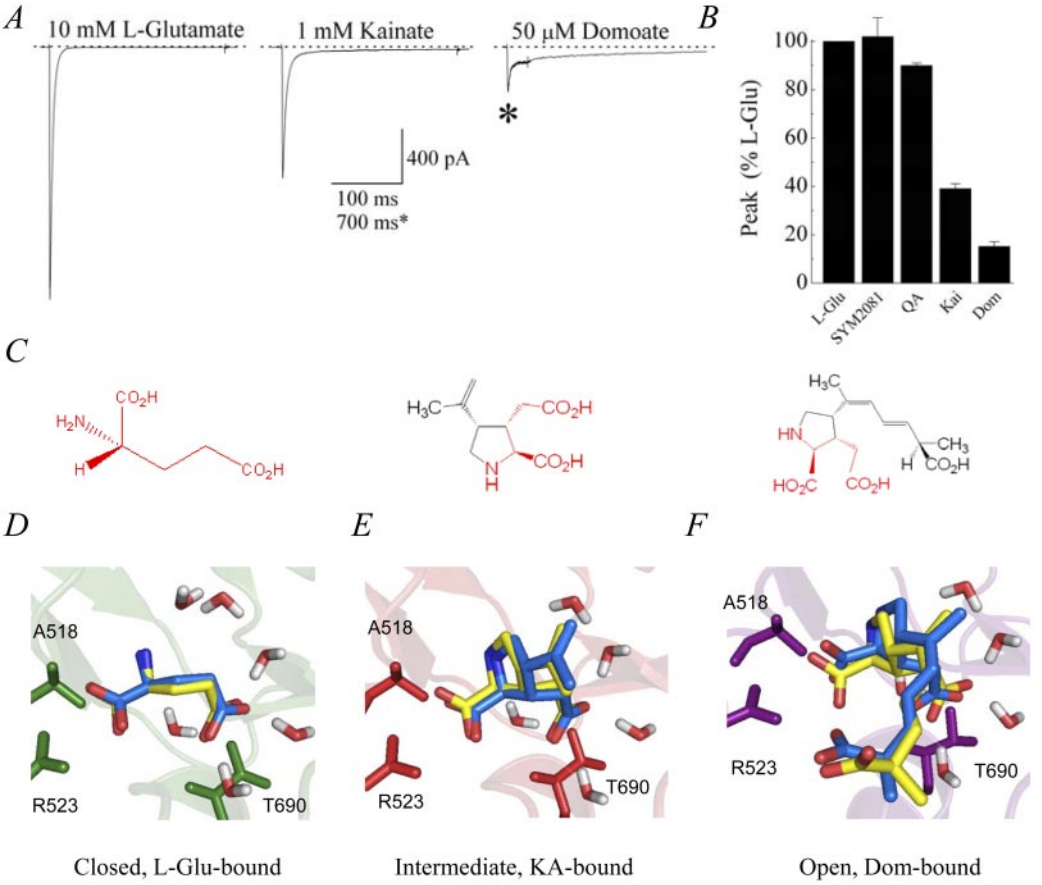

Fig. 4. FITTED accurately predicts conformations adopted by the GluK2 agonist-binding domain. A, membrane currents evoked by L-Glu (10 mM, 250-ms duration, H_p = −20 mV), KA (1 mM), and Dom (50 μM) in the same outside-out patch containing homomeric GluK2 channels (patch number 030724p2). *, Dom response is drawn on a different time base. B, summary plot showing peak responses evoked by five agonists, all of which have been cocrystallized with the GluK2 KAR: L-Glu (n = 13), SYM 2081 (n = 3), QA (n = 3), KA (n = 13), and Dom (n = 8). All data are expressed as the mean ± S.E.M. C, extended molecular structures showing that kainate and domoate have a common L-Glu backbone (red labeling). D to F, superimposition of the GluK2 agonist-binding pocket containing L-Glu, KA, and Dom where the solved crystal structures are compared with that docked by FITTED. In this and subsequent figures, the numbering of amino acid residues begins at the start site of the open reading frame and therefore includes the signal peptide. The solved crystal structures are shown in yellow, whereas the modeled structures are in blue. Key residues as well as agonist and water molecules are shown as sticks. L-Glu, KA, and Dom selected the closed (green), intermediate (red), and the open conformations (purple), respectively. Note that binding of KA and Dom displaces one of the key surrogate water molecules, which are present in the L-Glu-bound crystal. Nonpolar hydrogens are omitted for clarity.

has shown that Dom induces domain closure of 12.3°, KA elicits an intermediate closure of 23.3°, whereas the degree of domain closure with SYM 2081, QA, and L-Glu are between 26.2° to 26.6° (Mayer, 2005; Nanao et al., 2005). Consequently, our electrophysiological data support the current view that agonist efficacy is determined by the degree of closure in the GluK2 ABD (Mayer, 2005; Nanao et al., 2005).

To look at domain closure and binding mode, we performed in silico ligand-docking with the same series of receptor agonists using FITTED (Fig. 4, D–F). FITTED is a suite of programs that is unique in that the fitting process permits flexibility in macromolecules (side chains and main chains) and the presence of bridging water molecules while treating protein/ligand complexes as realistic dynamic systems (Corbeil et al., 2007). These characteristics are particularly relevant to the iGluR ABD because ligand and protein flexibility as well as water molecule mobility are critical determinants of agonist behavior (Arinaminpathy et al., 2006). In practical terms, agonists were docked to previously published structures of GluK2 that together represent the closed, intermediate or open conformation of the ABD (see *Materials and Methods* for details). It is important to emphasize that the final structure only ever represents a composite of these input structures and that FITTED cannot predict a completely novel structure. Upon convergence of the fitting process, we were able to assign a preferred conformation of the GluK2 ABD to each agonist.

In agreement with published X-ray crystal structures (Mayer, 2005; Nanao et al., 2005), the full agonist, L-Glu, selected the closed conformation (Fig. 4D), whereas the partial agonists, KA and Dom, selected intermediate and open conformations, respectively. Superimposition of the agonist-receptor complexes observed with FITTED and published X-ray crystal structures reveal that the structures obtained by each approach were indistinguishable (Fig. 4, D–F). In support of this, comparison of the computed RMSDs between the crystal and docked structures for L-Glu, KA and Dom were 0.34, 0.46, and 1.2 Å, respectively (Table 1) indicating that the ligand pose was accurately selected for each agonist. A closer view of the GluK2 ligand-binding pocket (Fig. 4, D–F) reveals key water molecules and selected amino acid residues involved in ligand recognition. For example, Arg523 and Ala518 are involved in H-bonding with the α-carboxyl group of all ligands. In contrast, Thr690 is involved in both direct hydrogen bonding with the γ-carboxyl group and indirect interactions through surrogate water molecules. Two other full agonists previously crystallized, SYM 2081 and QA, also selected the closed clamshell conformation with small computed RMSDs (SYM 2081, 0.24 Å; QA, 2.0 Å; Table 1). Taken together, our findings validate the use of FITTED in providing information on the conformational state adopted by the GluK2 ABD bound by different receptor agonists.

Agonist Efficacy and Predictions of Domain Closure Do Not Correlate. We next broadened our analysis to include all L-Glu analogs. With the exception of KA and Dom, FITTED predicted that all amino acids bind preferentially to the closed conformation, suggesting that agonist efficacy and the degree of closure in the GluK2 ABD are apparently not correlated (Fig. 5). At first glance, this result was perplexing, because it suggests that weak partial agonists, such as stereoisomers of Asp or Ser, elicit similar degrees of conformational change as L-Glu (Fig. 5B). Our immediate concern was

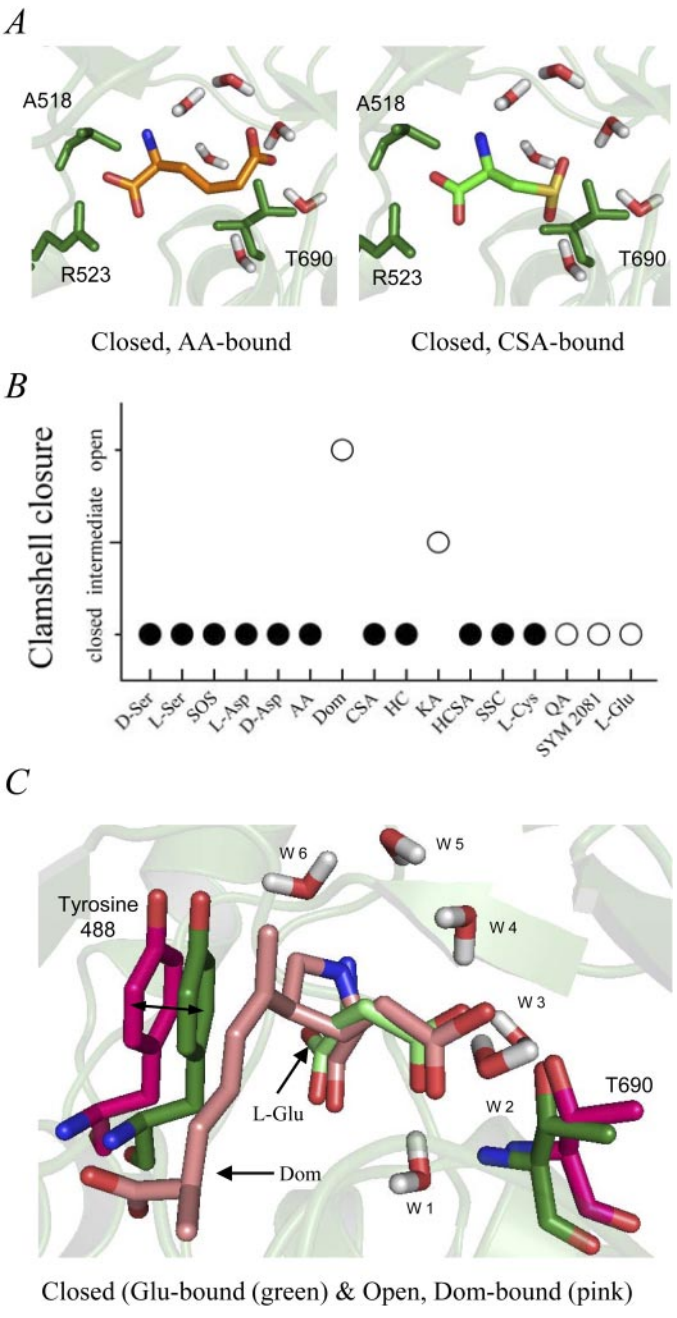

Fig. 5. Tyrosine 488 prevents full cleft closure with domoate and kainate. A, docking of L-aminoadipate (AA; left) and CSA (right) to GluK2 KARs using FITTED selects the closed conformation (green) in each case. The modeled structures are shown in orange and green, respectively. B, summary plot showing the conformation selected by each L-Glu analog using FITTED. Agonists previously cocrystallized with GluK2 are labeled as open circles, whereas the conformation selected by newly identified ligands is denoted by a filled circle. C, superimposition of the GluK2 ABD in complex with L-Glu (green) and Dom (pink). Note that different shading intensities have been used to distinguish between amino acid residues in the GluK2 ABD from the agonist molecule. In addition, only the protein backbone of the closed conformation is illustrated. Note that the pyrrolidine ring of Dom elicits a displacement of the Tyr488 residue as well as a water molecule (W6) normally found in the L-Glu-bound crystal structure. It is noteworthy that KA has the same effect though to a lesser extent because of to its smaller side-chain that extends from the pyrrolidine ring. Agonists, water molecules, and selected key residues are shown as sticks. Nonpolar hydrogens have been omitted for clarity.

that the outcome of the modeling represented a local minimum in the fitting process that is nonsensical from a biological perspective. However, we excluded this on two counts. First, FITTED already predicted the correct docking orientation of ligands previously crystallized with the GluK2 ABD (see Figure 4). Second, the binding mode of all other docked agonists was comparable with the binding orientation observed with L-Glu as would be expected. Typical binding orientation is illustrated by a visual inspection of the GluK2 ligand-binding pocket docked with L-α-aminoadipate and L-homocysteine sulfinic (Fig. 5A). In each case, the α-carboxyl groups of both partial agonists are predicted to form H-bonds with Ala518, Arg523, and AlaA689 (Fig. 5A), whereas the α-amino group is predicted to interact with Pro516 and Glu738 (data not shown). As expected, FITTED predicts that the terminal-carbon interacts with Thr690 via direct H-bonding and surrogate water molecules.

An additional concern was that the limited number of structures of the KAR ABD may bias the outcome of our analysis with FITTED. Although important to consider, we feel that this issue is not critical in our case, because the structures we have used cover an appreciable range of cleft closure in the GluK2 ABD from 12.3° for Dom to 26.2° to 26.6° for L-Glu (Mayer, 2005; Nanao et al., 2005). Furthermore, these structures represent the preferred conformations of full agonists (i.e., L-Glu, SYM 2081, and QA) to moderate and weak partial agonists (e.g., KA, Dom). FITTED does not provide information on whether the ABD adopts discrete or a limitless range of conformations after agonist binding. Nor does it identify any putative twist motion proposed from molecular dynamics to occur with partial agonists acting on GluA2 AMPARs (Bjerrum and Biggin, 2008). However, given these limitations, FITTED still permits us to examine the more general issue of whether there is any proposed relationship between cleft closure and agonist efficacy.

It is not wholly surprising that FITTED predicts that weak partial agonists, such as Asp or Ser, elicit the same degree of domain closure as full agonists, such as L-Glu, especially because almost all ligands used in this study have compact structures. Consequently, it is reasonable that most of the agonists we have docked using FITTED prefer the closed rather than the open or intermediate conformation of the KAR ABD. This conclusion is supported by recent work on AMPARs that has established the precedence that agonist efficacy need not be correlated with the degree of cleft closure (Zhang et al., 2008). Specifically, Zhang et al. (2008) found that mutation of the Thr686 residue of the GluA2 AMPAR renders L-Glu a partial agonist but yet structural changes elicited are indistinguishable from wild-type receptors. The exceptions to this at GluK2 receptors are KA and Dom, which prefer the intermediate and open conformations. However, as explained below, this observation can be simply accounted for by steric hindrance within the KAR ABD that limits the closure achieved by more bulky ligands, such as KA and Dom.

Domain Closure Is Determined by Ligand Interaction with Tyrosine 488. If the degree of closure in the ABD is not correlated with agonist efficacy, what is the basis for differences in closure observed with some agonists? Visual inspection of the ligand-bound complexes predicted by FITTED reveals an important property of the GluK2 ABD unique to Dom- and KA-bound structures (Fig. 5C). Specifically, the large side chain that extends from position 4 on the pyrrolidine ring of Dom causes a translational motion of Tyr488 that prevents complete closure of the GluK2 ABD. Likewise, the shorter side chain extending from the pyrrolidine ring of KA also causes steric hindrance but to a lesser extent accounting for the intermediate closure of the ABD. In contrast, all other amino acids tested, including the full agonist L-Glu, do not interact directly with Tyr488 and, because of their compact structure, allow complete closure of the agonist-binding pocket (Fig. 5B). The exception to this is QA, which possesses a bulky oxadiazolidine ring (Fig. 1). In this case, however, the ring structure of QA occupies a different region of the GluK2 ABD from the pyrrolidine ring of Dom and KA. Consequently, QA binds to GluK2 permitting complete closure of the ABD.

Conformational Changes Elicited by D- and L-Asp Are Indistinguishable from L-Glu. Although docking experiments with FITTED predicts that weak partial agonists, such as D- and L-Asp, bind to the closed conformation of the GluK2 ABD, it was nevertheless important to demonstrate this experimentally. To do this, we examined GluK2 responses after pretreatment with Con-A (Fig. 6). Con-A binds to a number of *N*-glycosylated residues in and around the GluK2 ABD (Fay and Bowie, 2006). In the resting or apo state of the GluK2 ABD, access to these sites is unrestricted; as a result, Con-A can bind to the receptor. Con-A binding in turn leads to the up-regulation of GluK2 responses as we have described previously (Bowie et al., 2003; Fay and Bowie, 2006). A typical experiment showing this effect is illustrated in Fig. 6A. Note that the equilibrium/peak response ratio to 10 mM L-Glu increased to 21.8 ± 2.9% after pretreatment with Con-A (10 μM, 3 mins) (Fig. 6, A and C). Conversely, if appreciable conformational changes are induced in the GluK2 ABD, such as occurs after L-Glu binding (Fay and Bowie, 2006), Con-A access to its binding sites are significantly restricted. As a consequence, pretreatment with Con-A has only a modest effect on the GluK2 response. In the example shown in Fig. 6A, the equilibrium/peak response ratio to L-Glu observed after pretreatment with Con-A was increased only to 6.7 ± 1.8% (Fig. 6, A and C).

State-dependent modulation by Con-A was therefore used to report the conformational changes elicited by D- and L-Asp. As positive controls, we compared the amount of modulation observed when GluK2 receptors were preincubated with Con-A and one of three agonists (i.e., 10 mM L-Glu, 1 mM KA, or 50 μM Dom) (Fig. 6, A and C). We have shown previously that Con-A modulation of GluK2 receptors preincubated with Glu, KA, or Dom corresponds to the closed, intermediate, or open states of the ABD, respectively (Fay and Bowie, 2006) (Fig. 6C). As negative controls, we examined pharmacological compounds that would not be expected to induce significant closure of the GluK2 ABD that were the competitive antagonist, 6-cyano-7-nitroquinoxaline-2,3-dione (CNQX), as well as the ion-channel blocker philanthotoxin (PhTX). Although CNQX induces modest closure in the AMPAR ABD by acting as a partial agonist (Menuz et al., 2007), this effect has not been observed at KARs; consequently, we have assumed it behaves as a competitive antagonist.

As expected, preincubation with CNQX or PhTX did not interfere with the degree of modulation of GluK2 receptors by Con-A (Fig. 6, B and C). In support of this, the degree of Con-A modulation observed with CNQX or PhTX was similar

to that observed for the open conformation of the GluK2 ABD but statistically distinct from the closed or intermediate (Table 2). These findings suggest that occupancy of the pore with a channel blocker or the ABD with a competitive antagonist does not evoke appreciable closure of the GluK2 ABD. In contrast, preincubation with either D- or L-Asp significantly reduced the degree of Con-A modulation (Fig. 6, B and C). In support of this, the degree of Con-A modulation observed with D-Asp or L-Asp was similar to that observed for the closed conformation of the GluK2 ABD but statistically distinct from the open or intermediate (Table 2). This finding further supports the central tenet of our study that weak partial agonists, such as D- and L-Asp, elicit conformational changes in the GluK2 ABD that are indistinguishable from conformations elicited by the full agonist, L-Glu.

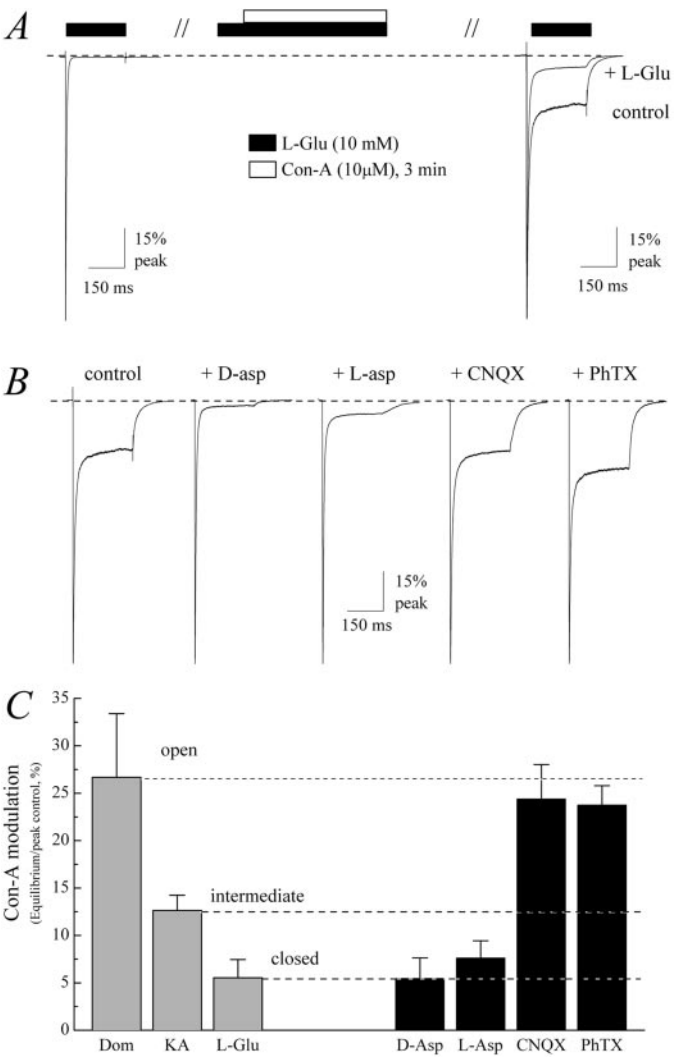

Fig. 6. Conformational changes elicited by L-Glu and stereoisomers of Asp to the GluK2 agonist-binding pocket are indistinguishable. A, typical experiment showing how modulation by Con-A reports conformational changes in the GluK2 ABD (for details, see Fay and Bowie, 2006). Con-A binds to a number of *N*-glycosylated residues in and around the GluK2 ABD. If agonist is bound, access to these sites is restricted; as a result, Con-A has a much weaker effect on the L-Glu equilibrium response. In the example shown, the equilibrium response is much smaller after coapplication of Con-A and L-Glu (10 mM; patch number 030724p2) than when Con-A is applied alone (control; patch number 01817p6). Filled and open bars indicate the application period of 10 mM L-Glu and 10 μM Con-A, respectively. The dotted line denotes the zero current level. The first and third applications of 10 mM Glu had a duration of 250 ms. B, experimental traces showing the extent of Con-A modulation as described in A, with D-Asp (patch number 071018p3), L-Asp (patch number 07906p1), CNQX (patch number 07913p2), and philanthotoxin (PhTX, patch number 07104p1) compared with control. C, Summary bar graphs showing the extent of Con-A modulation after cotreatment with various pharmacological agents (L-Glu, $n = 13$; D-Asp, $n = 4$; L-Asp, $n = 4$; CNQX, $n = 3$; PhTX, $n = 3$). The dotted lines on the graph denote the extent of Con-A modulation observed for the open, intermediate, and closed conformations of the GluK2 ABD, which we have described previously (A.-M.L. Fay and D. Bowie, 2006). CNQX and PhTX adopt the open conformation of the GluK2 ABD because their degree of Con-A modulation exactly matches that observed with Dom. In contrast, both D- and L-Asp adopt the closed conformation because modulation with Con-A is statistically indistinguishable from that observed with L-Glu. All data are expressed as the mean ±S.E.M.

Although these observations are consistent with Con-A reporting conformational changes in the GluK2 ABD, it was nevertheless important to evaluate alternate explanations. For example, it is possible that Con-A modulation reveals that stereoisomers of Asp adopt a desensitized conformation similar to that L-Glu instead of reporting the extent of cleft closure. This possibility, however, is unlikely for three main reasons. First, there is no available evidence to suggest that conformational changes in the dimer interface that accompany the onset of AMPA or KAR desensitization are agonist-dependent (Armstrong et al., 2006; Weston et al., 2006), which would be required to explain Con-A's effects. Second, Con-A binding and consequently modulation of GluK2 is almost entirely eliminated by mutation of three key N-terminal amino acid residues that do not participate in forming the dimer interface (Fay and Bowie, 2006). Although residues distant from the dimer interface may still regulate KAR desensitization, GluK2 receptors that lack the N-terminal desensitize normally (Plested and Mayer, 2007), suggesting that this region of the intact receptor is not functionally coupled to the dimer interface. Third and finally, Con-A does not affect rates into or out of desensitization (Bowie et al., 2003; Fay and Bowie, 2006), which would not be expected if lectin binding reports separation in the dimer interface. Given this, the most parsimonious explanation of our data is that Con-A reports conformational changes in the ABD of GluK2 receptor as discussed in detail elsewhere (Fay and Bowie, 2006).

Discussion

To our knowledge, this study is the first to identify a series of structurally related amino acids that exhibit the entire range of agonist behavior at KARs. Analysis of their struc-

TABLE 2
Statistical comparisons between the degree of Con-A modulation observed with different GluK2 receptor ligands

The ability of stereoisomers of Asp, CNQX, and PhTX to affect Con-A modulation of GluK2 receptors was compared with the modulation observed with L-Glu, KA, and Dom using Student's *t* test. The modulation observed by preincubating with stereoisomers of Asp was statistically significant from that observed with KA and Dom but indistinguishable from L-Glu. In contrast, the modulation observed by pre-incubating with CNQX or PhTX was statistically significant from that observed with L-Glu and KA but indistinguishable from Dom.

Ligand	L-Glu (Closed)	KA (Intermediate)	Dom (Open)
D-Asp	N.S.	*	*
L-Asp	N.S.	*	*
PhTX	**	**	N.S.
CNQX	**	**	N.S.

N.S., not significant.
* Significant at $P < 0.05$.
** Significant at $P < 0.01$.

ture-function relationship reveals that the agonist binding pocket of KARs is ideally suited to respond to the neurotransmitter, L-Glu, because modest changes in its chain length generates weak partial agonists. Using both in silico docking as well as measurements of conformations in the intact receptor, we show that the majority of full and partial agonists select for the closed conformation of the GluK2 ABD. Although this finding is not wholly surprising given the compact structures of most ligands tested, it is inconsistent with agonist efficacy being solely determined by the extent of closure in the KAR ABD. Exceptions to this were the partial agonists, KA and Dom, which select for the open and intermediate conformations, respectively. However this finding can be simply explained by steric hindrance due to the Tyr 488 residue in domain 1 of the GluK2 ABD. Our findings suggest the value in looking more closely at the relationship between agonist efficacy and the extent of agonist-induced domain closure in KARs.

Can Other Mechanisms Account for Agonist Efficacy at Kainate Receptors? Although the view that agonist efficacy is governed by closure in the ABD has gained much popularity, recent work on AMPARs has identified a different mechanism (though not mutually exclusive) (Robert et al., 2005; Zhang et al., 2008) that may also account for full and partial agonist behavior at KARs. In essence, it is argued that the time the ABD remains in the closed conformation determines several gating properties of AMPARs including agonist efficacy, deactivation rates as well as apparent agonist affinity. For L-Glu, closed-cleft stability is optimized by direct and indirect interactions with domains 1 and 2 of the AMPAR ABD, which permit L-Glu to attain full agonist activity while exhibiting rapid unbinding (Robert et al., 2005; Zhang et al., 2008), essential features for any fast-acting neurotransmitter. In the specific case of AMPARs, mutation of a key threonine (i.e., Thr686) residue in domain 2 of the GluR2 ABD, disrupts the optimization established between the ligand and receptor. As a result, L-Glu is rendered a weak partial agonist with much lower affinity (Robert et al., 2005).

There are several reasons to suggest that basic elements of the mechanism proposed by Zhang et al. (2008) may also account for differences in efficacy between L-Glu and stereoisomers of Asp reported in this study. First, activation curves of partial agonists D- and L-Asp are shifted rightward compared with the full agonist L-Glu (Fig. 3, C and D), suggesting that, in this case, agonist efficacy and affinity may be tightly correlated. Second, deactivation rates for stereoisomers of Asp (e.g., D-Asp, $\tau = 1.2 \pm 0.3$ ms) were faster than with L-Glu ($\tau = 2.6 \pm 0.2$ ms) (Bowie, 2002). Third and finally, the more extended structure of L-Glu permits more contact points (direct and indirect) to be established with the GluK2 ABD than with D- or L-Asp (Fig. 7). This difference in agonist binding would be expected to weaken the stability of the closed GluK2 ABD. It is noteworthy that L-Asp formed considerably less contacts than D-Asp or L-Glu, which may explain its weaker responsiveness based on analysis of activation curves (Fig. 3D). Although more work is required to rigorously test this model, it provides a valuable framework for future work on agonist behavior at KARs.

Are Amino Acids Other Than L-Glu Suitable Neurotransmitter Candidates at Kainate Receptors? Several of the amino acids examined in this study are endogenous to the CNS and have been previously evaluated as neurotrans-

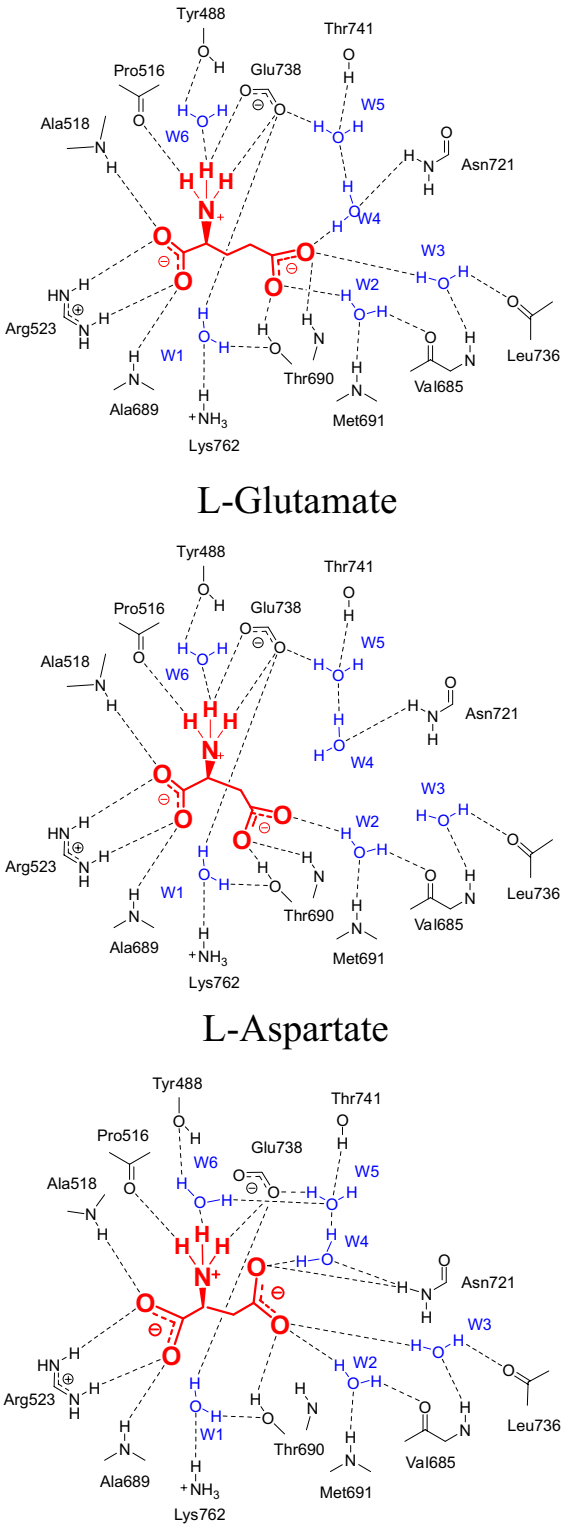

Fig. 7. Stereoisomers of Asp establish fewer contact points with the GluK2 agonist binding pocket than L-Glu. Two-dimensional topographical maps of the GluK2 ABD shows that the number of contact points and the binding orientation of the full agonist, L-Glu, and partial agonists, D- and L-Asp. Topographical maps were deduced from structure complexes obtained with FITTED. Note the number of contact points made by D- and L-Asp was fewer than with L-Glu. In addition, the binding orientation is different between L- and D-Asp, which would be expected for stereoisomers of the same amino acid.

mitter candidates at glutamatergic synapses. The candidature of sulfur-containing amino acids, which include L-Cys, HC, SSC, and HCSA, was considered after mechanisms that lead to their release, uptake, and responsiveness (see below) were identified (Do et al., 1986; Bouvier et al., 1991). Recent attention has focused on their potent activation of metabotropic glutamate receptors (e.g., Kingston et al., 1998). However, earlier work demonstrated that they also activate iGluRs (Thompson and Kilpatrick, 1996). At the time, most investigators argued for their greater ability to activate NMDARs than AMPARs (Patneau and Mayer, 1990); however, their effect on KARs was never tested, because evidence for the existence of this iGluR subclass had yet to emerge (Bowie, 2008). In view of this, our data on homomeric GluK2 receptors suggests the value in testing the responsiveness of native KARs to sulfur-containing amino acids. It is noteworthy that the most potent sulfur-containing amino acid in our experiments, L-Cys, is a very weak partial agonist on homomeric GluR1 AMPARs (A.-M.L. Fay and D. Bowie, unpublished observations). Therefore, it would be interesting in future work to determine whether different non-NMDA receptor subtypes discriminate among sulfur-containing amino acids.

In comparison, there is more compelling evidence linking the stereoisomers of both serine and aspartate to roles in glutamatergic transmission (Boehning and Snyder, 2003). D-Ser was considered in this capacity only after it was shown to act as a coagonist at the glycine binding site of NMDARs (McBain et al., 1989). Because D-serine is expressed in discrete populations of glial cells opposed to NMDARs (Schell et al., 1997a), it has been categorized as a gliotransmitter (Mothet et al., 2000; Panatier et al., 2006). The role of D-Asp is more elusive, although it is found in the developing and adult brain (Schell et al., 1997b). Accumulation of D-Asp in CNS tissue has marked behavioral consequences, such as impaired motor coordination (Weil et al., 2006), which is consistent with its putative role as a transmitter at the climbing fibers of the cerebellum (Wiklund et al., 1982). Likewise, L-Asp's role in neurotransmission has centered on NMDARs (Fleck et al., 1993), although it elicits a high calcium conductance in cerebellar Purkinje cells that apparently involves a novel iGluR (Yuzaki et al., 1996). Our study shows that D- and L-forms of each amino acid are weak partial agonists and, although these properties are not normally expected of a neurotransmitter candidate, it may be interesting to evaluate their roles at native KAR-containing synapses.

Conclusion

It is puzzling that not all iGluR subunits respond to the neurotransmitter L-Glu. In fact, neither the NR1 NMDAR subunit nor the orphan-class δ-2 (δ2) subunit even binds L-Glu. Because the ancestral iGluR, GluR0, possesses an L-Glu binding pocket (Chen et al., 1999), it is conceivable that evolving NR1 and δ2 subunits sacrificed this ability to serve more specialized roles in the mammalian CNS. In this regard, it is interesting that NMDARs (McBain et al., 1989) and orphan-class δ2 iGluR (Naur et al., 2007) retained their ability to bind D-Ser. Likewise, AMPARs (P. Brown and D. Bowie, unpublished observations) and KARs (present study) are also gated by D-Ser (and D-Asp) suggesting that these naturally occurring D-amino acids discriminate little among iGluR families. Whether this observation is a peculiarity of iGluRs that holds little biological significance or hints at a broader role for D-amino acids at glutamatergic synapses awaits future investigation.

Acknowledgments

We are grateful to David MacLean, Mark Aurousseau, and Elizabeth Andrews for discussions during the course of this work and Drs. G. Miller and R. Blunck for comments on the manuscript. We thank the Réseau québécois de calcul de haute performance for allocation of computer resources for this study.

References

Arinaminpathy Y, Sansom MS, and Biggin PC (2006) Binding site flexibility: molecular simulation of partial and full agonists within a glutamate receptor. *Mol Pharmacol* **69:**11–18.
Armstrong N and Gouaux E (2000) Mechanisms for activation and antagonism of an AMPA-sensitive glutamate receptor: crystal structures of the GluR2 ligand binding core. *Neuron* **28:**165–181.
Armstrong N, Jasti J, Beich-Frandsen M, and Gouaux E (2006) Measurement of conformational changes accompanying desensitization in an ionotropic glutamate receptor. *Cell* **127:**85–97.
Bjerrum EJ and Biggin PC (2008) Rigid body essential X-ray crystallography: distinguishing the bend and twist of glutamate receptor ligand binding domains. *Proteins* **72:**434–446.
Boehning D and Snyder SH (2003) Novel neural modulators. *Annu Rev Neurosci* **26:**105–131.
Bouvier M, Miller BA, Szatkowski M, and Attwell D (1991) Electrogenic uptake of sulphur-containing analogues of glutamate and aspartate by muller cells from the salamander retina. *J Physiol* **444:**441–457.
Bowie D (2002) External anions and cations distinguish between AMPA and kainate receptor gating mechanisms. *J Physiol* (*Lond*) **539:**725–733.
Bowie D (2008) Ionotropic glutamate receptors & CNS disorders. *CNS Neurol Disord Drug Targets* **7:**129–143.
Bowie D, Garcia EP, Marshall J, Traynelis SF, and Lange GD (2003) Allosteric regulation and spatial distribution of kainate receptors bound to ancillary proteins. *J Physiol* (*Lond*) **547:**373–385.
Chen GQ, Cui C, Mayer ML, and Gouaux E (1999) Functional characterization of a potassium-selective prokaryotic glutamate receptor. *Nature* **402:**817–821.
Collingridge GL, Olsen RW, Peters J, and Spedding M (2009) A nomenclature for ligand-gated ion channels. *Neuropharmacology* **56:**2–5.
Corbeil CR, Englebienne P, and Moitessier N (2007) Docking ligands into flexible and solvated macromolecules. 1. Development and validation of FITTED 1.0. *J Chem Inf Model* **47:**435–449.
Do KQ, Mattenberger M, Streit P, and Cuénod M (1986) In vitro release of endogenous excitatory sulfur-containing amino acids from various rat brain regions. *J Neurochem* **46:**779–786.
Fay AM and Bowie D (2006) Concanavalin-A reports agonist-induced conformational changes in the intact glur6 kainate receptor. *J Physiol* **572:**201–213.
Fleck MW, Henze DA, Barrionuevo G, and Palmer AM (1993) Aspartate and glutamate mediate excitatory synaptic transmission in area CA1 of the hippocampus. *J Neurosci* **13:**3944–3955.
Inanobe A, Furukawa H, and Gouaux E (2005) Mechanism of partial agonist action at the NR1 subunit of NMDA receptors. *Neuron* **47:**71–84.
Jin R, Banke TG, Mayer ML, Traynelis SF, and Gouaux E (2003) Structural basis for partial agonist action at ionotropic glutamate receptors. *Nat Neurosci* **6:**803–810.
Kingston AE, Lowndes J, Evans N, Clark B, Tomlinson R, Burnett JP, Mayne NG, Cockerham SL, and Lodge D (1998) Sulphur-containing amino acids are agonists for group 1 metabotropic receptors expressed in clonal RGT cell lines. *Neuropharmacology* **37:**277–287.
Mayer ML (2005) Crystal structures of the glur5 and glur6 ligand binding cores: molecular mechanisms underlying kainate receptor selectivity. *Neuron* **45:**539–552.
McBain CJ, Kleckner NW, Wyrick S, and Dingledine R (1989) Structural requirements for activation of the glycine coagonist site of *N*-methyl-D-aspartate receptors expressed in *Xenopus* oocytes. *Mol Pharmacol* **36:**556–565.
Menuz K, Stroud RM, Nicoll RA, and Hays FA (2007) TARP auxiliary subunits switch AMPA receptor antagonists into partial agonists. *Science* **318:**815–817.
Mothet JP, Parent AT, Wolosker H, Brady RO Jr, Linden DJ, Ferris CD, Rogawski MA, and Snyder SH (2000) D-Serine is an endogenous ligand for the glycine site of the *N*-methyl-D-aspartate receptor. *Proc Natl Acad Sci U S A* **97:**4926–4931.
Nanao MH, Green T, Stern-Bach Y, Heinemann SF, and Choe S (2005) Structure of the kainate receptor subunit GluR6 agonist-binding domain complexed with domoic acid. *Proc Natl Acad Sci U S A* **102:**1708–1713.
Naur P, Hansen KB, Kristensen AS, Dravid SM, Pickering DS, Olsen L, Vestergaard B, Egebjerg J, Gajhede M, Traynelis SF, et al. (2007) Ionotropic glutamate-like receptor delta2 binds D-serine and glycine. *Proc Natl Acad Sci U S A* **104:**14116–14121.
Panatier A, Theodosis DT, Mothet JP, Touquet B, Pollegioni L, Poulain DA, and Oliet SH (2006) Glia-derived D-serine controls NMDA receptor activity and synaptic memory. *Cell* **125:**775–784.
Patneau DK and Mayer ML (1990) Structure-activity relationships for amino acid

transmitter candidates acting at *N*-methyl-D-aspartate and quisqualate receptors. *J Neurosci* **10:**2385–2399.
Plested AJ and Mayer ML (2007) Structure and mechanism of kainate receptor modulation by anions. *Neuron* **53:**829–841.
Robert A, Armstrong N, Gouaux JE, and Howe JR (2005) AMPA receptor binding cleft mutations that alter affinity, efficacy, and recovery from desensitization. *J Neurosci* **25:**3752–3762.
Schell MJ, Brady RO, Jr., Molliver ME, and Snyder SH (1997a) D-Serine as a neuromodulator: regional and developmental localizations in rat brain glia resemble NMDA receptors. *J Neurosci* **17:**1604–1615.
Schell MJ, Cooper OB, and Snyder SH (1997b) D-Aspartate localizations imply neuronal and neuroendocrine roles. *Proc Natl Acad Sci U S A* **94:**2013–2018.
Stern-Bach Y, Bettler B, Hartley M, Sheppard PO, O'Hara PJ, and Heinemann SF (1994) Agonist-selectivity of glutamate receptors is specified by two domains structurally related to bacterial amino acid binding proteins. *Neuron* **13:**1345–1357.
Thompson GA and Kilpatrick IC (1996) The neurotransmitter candidature of sulphur-containing excitatory amino acids in the mammalian central nervous system. *Pharmacol Ther* **72:**25–36.
Weil ZM, Huang AS, Beigneux A, Kim PM, Molliver ME, Blackshaw S, Young SG, Nelson RJ, and Snyder SH (2006) Behavioural alterations in male mice lacking the gene for D-aspartate oxidase. *Behav Brain Res* **171:**295–302.
Weston MC, Schuck P, Ghosal A, Rosenmund C, and Mayer ML (2006) Conformational restriction blocks glutamate receptor desensitization. *Nat Struct Mol Biol* **13:**1120–1127.
Wiklund L, Toggenburger G, and Cuénod M (1982) Aspartate: possible neurotransmitter in cerebellar climbing fibers. *Science* **216:**78–80.
Wong AY, Fay AM, and Bowie D (2006) External ions are coactivators of kainate receptors. *J Neurosci* **26:**5750–5755.
Yuzaki M, Forrest D, Curran T, and Connor JA (1996) Selective activation of calcium permeability by aspartate in purkinje cells. *Science* **273:**1112–1114.
Zhang W, Cho Y, Lolis E, and Howe JR (2008) Structural and single-channel results indicate that the rates of ligand binding domain closing and opening directly impact AMPA receptor gating. *J Neurosci* **28:**932–943.

Address correspondence to: Dr. Derek Bowie, Department of Pharmacology and Therapeutics, McIntyre Medical Sciences Building, Room 1317, McGill University, 3655 Promenade Sir William Osler, Montreal, Québec, Canada H3A 1Y6. E-mail: derek.bowie@mcgill.ca